

## SPECIAL ARTICLE

## Recommendations for the diagnosis and radiological follow-up of pituitary neuroendocrine tumours



Carmen Fajardo-Montañana<sup>a,\*</sup>, Rocío Villar<sup>b</sup>, Beatriz Gómez-Ansón<sup>c</sup>, Beatriz Brea<sup>d</sup>, Antonio Jesús Mosqueira<sup>e</sup>, Enrique Molla<sup>f</sup>, Joaquín Enseñat<sup>g</sup>, Pedro Riesgo<sup>h</sup>, Jorge Cardona-Arboniés<sup>i</sup>, Ovidio Hernando<sup>j</sup>

<sup>a</sup> Departamento de Endocrinología, Hospital Universitario de la Ribera, Alcira, Valencia, Spain

<sup>b</sup> Departamento de Endocrinología, Complejo Hospitalario Universitario de Santiago, Santiago de Compostela, A Coruña, Spain

<sup>c</sup> Neurorradiología, Departamento de Radiodiagnóstico, Hospital Universitari Sant Pau, Barcelona, Spain

<sup>d</sup> Departamento de Radiología, Hospital Universitario Puerta de Hierro, Majadahonda, Madrid, Spain

<sup>e</sup> Departamento de Radiología, Complejo Hospitalario Universitario de Santiago, Santiago de Compostela, A Coruña, Spain

<sup>f</sup> Departamento de Radiología, Hospital Universitario de la Ribera, Alcira, Valencia, Spain

<sup>g</sup> Departamento de Neurocirugía, Hospital Clínic de Barcelona, Barcelona, Spain

<sup>h</sup> Departamento de Neurocirugía, Hospital Universitario de la Ribera, Alcira, Valencia, Spain

<sup>i</sup> Departamento de Medicina Nuclear, Hospital Universitario Puerta de Hierro, Majadahonda, Madrid, Spain

<sup>j</sup> Departamento de Oncología Radioterápica, Centro Integral Oncológico Clara Campal, Madrid, Spain

Received 4 August 2021; accepted 1 October 2021

Available online 22 November 2022

### KEYWORDS

Neuroendocrine tumours;  
Neuroradiology;  
Diagnosis;  
Follow-up;  
Prognosis;  
Recommendations

**Abstract** Pituitary neuroendocrine tumours (PitNETs) constitute a heterogeneous group of tumours with a gradually increasing incidence, partly accounted for by more sensitive imaging techniques and more extensive experience in neuroradiology in this regard. Although most PitNETs are indolent, some exhibit aggressive behaviour, and recurrence may be seen after surgical removal. The changes introduced in the WHO classification in 2017 and terminological debates in relation to neuroendocrine tumours warrant an update of the guidelines for the diagnosis, pre-operative and postoperative management, and follow-up of response to treatment of PitNETs. This multidisciplinary document, an initiative of the Neuroendocrinology area of the Sociedad Española de Endocrinología y Nutrición [Spanish Society of Endocrinology and Nutrition] (SEEN), focuses on neuroimaging studies for the diagnosis, prognosis and follow-up of PitNETs. The basic requirements and elements that should be covered by magnetic resonance imaging are described, and a minimum radiology report to aid clinicians in treatment decision-making is proposed. This work supplements the consensus between the Neuroendocrinology area of the SEEN and the Sociedad Española de Anatomía Patológica [Spanish Society of Pathology] (SEAP) for the pathological study of PitNETs.

© 2021 The Author(s). Published by Elsevier España, S.L.U. on behalf of SEEN and SED. This is an open access article under the CC BY-NC-ND license (<http://creativecommons.org/licenses/by-nc-nd/4.0/>).

\* Corresponding author.

E-mail address: [fajardo\\_carmon@gva.es](mailto:fajardo_carmon@gva.es) (C. Fajardo-Montañana).

**PALABRAS CLAVE**

Tumores  
neuroendocrinos;  
Neurorradiología;  
Diagnóstico;  
Seguimiento;  
Pronóstico;  
Recomendaciones

**Recomendaciones sobre el diagnóstico y seguimiento radiológico de los tumores neuroendocrinos hipofisarios**

**Resumen** Los tumores neuroendocrinos hipofisarios (TNEH) constituyen un grupo heterogéneo de tumores cuya incidencia ha experimentado un aumento progresivo a la que han contribuido técnicas de imagen más sensibles y mayor experiencia en neurorradiología en este ámbito. Aunque la mayoría de los TNEH son indolentes, algunos presentan un comportamiento agresivo, y puede aparecer recurrencia tras la extirpación quirúrgica. Los cambios introducidos por la clasificación de la OMS en 2017 y las controversias terminológicas con relación a los tumores neuroendocrinos hacen necesario actualizar las recomendaciones para el diagnóstico, manejo pre- y postoperatorio y seguimiento de respuesta al tratamiento de los TNEH. Este documento multidisciplinar, iniciativa del área de Neuroendocrinología de la Sociedad Española de Endocrinología y Nutrición (SEEN), se centra en los estudios neurorradiológicos de imagen médica para el diagnóstico, pronóstico y seguimiento de los TNEH. Se describen los requisitos básicos y aspectos que deben cubrir los estudios con resonancia magnética nuclear, y se propone un informe mínimo de radiología que ayude al clínico en sus decisiones terapéuticas. Este trabajo complementa así el consenso entre el Área de Neuroendocrinología de la SEEN y de la Sociedad Española de Anatomía Patológica (SEAP) para el estudio anatomopatológico de los TNEH.

© 2021 El Autor(s). Publicado por Elsevier España, S.L.U. en nombre de SEEN y SED. Este es un artículo Open Access bajo la licencia CC BY-NC-ND (<http://creativecommons.org/licenses/by-nc-nd/4.0/>).

**Introduction**

Pituitary neuroendocrine tumours (PitNETs) constitute a heterogeneous group of tumours in radiological, histological and clinical terms<sup>1</sup>. In recent years, there has been a progressive increase in their incidence, justified by an increase in experience in expert neuroradiological examination and by the development of more sensitive imaging techniques<sup>2,3</sup>. PitNETs constitute 15–25% of intracranial neoplasms<sup>1,4–7</sup>; the most common are adenohypophyseal (85–90% of cases). However, in the sellar region, it is also possible to find other lesions, such as metastases of multiple origins, mesenchymal, meningeal or neural neoplasms, cysts, and inflammatory processes<sup>4–7</sup>. It is estimated that 15% of the population would present a tumour found by neuroimaging or pathological anatomy. PitNETs with clinical repercussions represent one out of every 1000<sup>8–10</sup>.

Although most PitNETs are indolent, with slow growth and an optimal response to treatment, some present aggressive behaviour (between 5% and 15% depending on the series<sup>11</sup>), characterised by local invasion, resistance to treatment and, very rarely, the appearance of metastases<sup>12</sup>. In addition, in some patients, despite surgical removal, recurrence occurs<sup>13</sup>. For all these reasons, the terminology used to define this group of tumours has been the subject of debate. Since 2016, the term PitNET has replaced the traditional concept of pituitary adenoma<sup>1</sup>. Regarding their classification, the most recent, carried out by the WHO in 2017, groups PitNETs according to the profile of pituitary hormones and transcription factors they express<sup>6</sup>. This classification has facilitated a different approach to their pathological diagnosis<sup>14,15</sup>. It has enabled a more precise classification of tumours, drastically reducing the percentage of null ones<sup>16–18</sup>.

The recent changes introduced in the WHO classification in 2017<sup>6</sup> and the terminological debate in relation to neuroendocrine tumours make it necessary to review the guidelines for the diagnosis, preoperative and postoperative management, and follow-up of response to treatment of PitNETs. Recently, a consensus has been drawn up between the Neuroendocrinology Knowledge Area of the Sociedad Española de Endocrinología y Nutrición (SEEN) [Spanish Society of Endocrinology and Nutrition] and the Sociedad Española de Anatomía Patológica (SEAP) [Spanish Society of Pathological Anatomy] for the anatomopathological study of PitNETs<sup>15</sup>. In a complementary manner, this multidisciplinary document, an initiative of the Neuroendocrinology area of the SEEN, focuses on neuroradiological imaging studies for the diagnosis, prognosis and follow-up of PitNETs.

**Magnetic resonance imaging (MRI) as the imaging test of choice in the study and follow-up of PitNETs**

Currently, MRI is considered the reference test in the imaging diagnosis of diseases of the hypothalamic-pituitary region<sup>8,19–21</sup>. With its higher contrast resolution and the possibility of obtaining multiplanar images, it enables the identification of normal structures, diagnosis of lesions, planning of surgical treatment, monitoring of pituitary disease and evaluation of response to treatment<sup>8</sup>.

**Indications for MRI in the diagnosis of PitNETs**

MRI is indicated for diagnosing various conditions where an anatomical or functional alteration of the pituitary gland is suspected. These include hyper- or hypofunction of the

adenohypophysis, dysfunction of the neurohypophysis, suspected compression of adjacent structures in the sellar region, the appearance of temporary visual field defects, or paralysis associated with cranial nerves III, IV, and VI.

#### Indications for other medical imaging techniques

**Computed axial tomography (CT).** CT was the technique used to study the pituitary region before the development of MRI, but the latter has displaced it due to its greater capacity for contrast resolution, avoiding the presence of beam hardening artifacts in the region of the sella turcica and exposure to ionising radiation from CT<sup>19</sup>. Therefore, CT is currently used for primary diagnosis only when MRI is contraindicated (e.g. some patients with pacemakers, ocular metallic foreign bodies, cochlear implants or obesity that technically precludes the use of MRI) and as a complement to MRI for the differential diagnosis of meningiomas, craniopharyngiomas and germinomas, since it allows the identification of calcifications or ossifications characteristic of these tumours. CT is also used to assess the bony integrity of the skull base and for surgical planning.

**Positron emission tomography (PET) with <sup>11</sup>C-methionine.** <sup>11</sup>C-methionine PET/CT (MET-PET/CT) is a sensitive and complementary technique to MRI to detect pituitary adenomas or residual tissue after pituitary surgery. The main advantage of MET-PET/CT over <sup>18</sup>F-fluorodeoxyglucose (FDG) lies in its better pituitary/brain uptake ratio<sup>22</sup>.

This modality has greater sensitivity, especially in recurrent microadenomas<sup>22</sup>. It can provide information when MRI or FDG are negative, especially in the case of microadenomas<sup>23,24</sup>. Its detection rate is higher than that of MRI in certain PitNETs<sup>25</sup>, and it is also useful for assessing the response to treatment with somatostatin analogues in these tumours<sup>23</sup>.

**Petrosal sinus catheterisation.** Petrosal sinus catheterisation is used in the diagnosis of Cushing's disease when the MRI image is inconclusive or in adenomas with a diameter of less than 6 mm<sup>26,27</sup>. Although it reaches sensitivities of over 90% to establish the pituitary origin of the disease, it is an invasive technique. It is not as specific in demonstrating the lateralisation of the tumour in one half or the other of the adenohypophysis<sup>28</sup>.

#### MRI requirements for the diagnosis and follow-up of PitNETs

##### Considerations on the power of MRI equipment

The pituitary gland does not usually measure more than 8 mm in length, and microadenomas can be very small, reaching no more than a millimetre in diameter. Therefore, it is essential that the images have good spatial resolution and optimal contrast resolution, that is, that they have an adequate signal-to-noise and contrast-to-signal ratio, respectively.

The first consideration when it comes to performing an MRI study of the pituitary on a 1.5 T or a 3 T scanner is the availability of each centre. Although there has been an increase in 3 T teams in recent years, they are still a minority, so indications for these scans must be carefully defined. Using equipment with a larger field may be useful if there is suspicion of a microadenoma, and the 1.5 T scanner does not

exclude this possibility<sup>29</sup>. It is also useful for more accurately assessing subtle differences between normal and abnormal tissue, predicting invasion of adjacent structures and evaluating the pituitary stalk<sup>29,30</sup>. However, high-field equipment poses technical difficulties, as it is more sensitive to artifacts, especially susceptibility artifacts, so they must be appropriately adjusted, and they pose greater limitations in some patients.

##### Use of contrast in MRI

Gadolinium contrast is used for MRI, both in the diagnosis and follow-up of pituitary lesions. Gadolinium contrast is used for MRI in the diagnosis and follow-up of pituitary lesions. For this reason, official reports have been issued on its use and restrictions<sup>31</sup>.

The clinical practice guidelines for PitNETs recommend a neuroradiological follow-up ranging from 3 to 12 months for aggressive tumours<sup>8</sup>. Still, they have not taken a position concerning non-aggressive ones. Clinicians need to be aware of the need to minimise patient exposure to gadolinium contrast<sup>32</sup>, adapt the interval between studies to each clinical situation, and avoid using contrast when it is unnecessary<sup>20,33</sup>.

#### Basic MRI protocol for the exploration of the neurohypophysis and the study of PitNETs

The pituitary MRI protocol can be divided into three parts<sup>21,34</sup>, described in [Table 1](#).

#### Structure and content of the radiology report of a pituitary MRI

An initial MRI scan report for suspected PitNETs should include all relevant information to define the lesion. [Table 2](#) is a proposed basic report based on the following points.

##### Morphological study

The first objective is to determine whether or not there is an alteration in the normal anatomy of the pituitary gland. In this way, the following should be taken into account: the volume and morphology of the sella, the size, signal and shape of the gland, the suprasellar content (stalk [[Fig. 1A](#)], chiasm and floor of the third ventricle) and the cavernous sinuses.

It should be remembered that the pituitary size is greater in neonates and women, especially in the pubertal period or during pregnancy and postpartum, where the shape of the pituitary with a convex superior border should not be confused with a pituitary adenoma. In some cases, primary glandular deficiencies can also be associated with physiological growth of the pituitary gland, for example, in the case of primary hypothyroidism<sup>35</sup>. Therefore, when faced with an anatomical alteration, it must be evaluated whether it is a normal variant or a lesion<sup>36</sup> ([Fig. 1B](#)).

**Table 1** Basic MRI protocol for the examination of neurohypophysis and study of PitNETs.

Study	Acquisition	Methodology	Objective
Morphological study	Routinely, sagittal and coronal plane sequences are performed, and very occasionally axial ones, enhanced on T1, without and with contrast, and on T2.	Fine slice sequence with high spatial resolution and a good signal-to-noise ratio. The cut should be fine, with a thickness between 2 and 3 mm. Can be reduced to 1 mm or 1.5 mm on 3 T equipment. Small field of view, between 140 and 160 mm.	Identify normal or pathological structures, their relationship with neighbouring structures, and determine whether they are solid, cystic, with a fatty, haemorrhagic or protein component. Distinguish areas with a high content of free water because they are hyperintense (ventricles, basal cisterns or cystic lesions). Delimit the intracranial vessels (carotids or the circle of Willis), hypointense due to the rapid flow of blood. Identify haemorrhagic content (e.g. hypointense signal on T2 in the pituitary). Very useful if the use of gadolinium contrast is contraindicated.
Dynamic study	Series of coronal T1-weighted images during the arterial phase of gadolinium administration.	A fast repetitive scan (low resolution) is performed, with coronal sequences in 10 min cycles. During the first sequence, a bolus of 10 ml at 2.5 ml/s + bolus of 20 ml of physiological serum is administered. The successive sequences make it possible to check how the signal intensity of the gland increases over time.	Identify a microadenoma by its slower enhancement than the rest of the pituitary tissue. The pituitary gland and pituitary stalk lack a blood-brain barrier, resulting in rapid and progressive enhancement that begins at the top of the gland and spreads to the rest.
Post-contrast study	Sagittal and coronal T1-weighted spin echo slices.		Observe the normal homogeneous enhancement that should appear in the late phase after administering gadolinium.

### Origin of the pituitary lesion

For the differential diagnosis, it is necessary to determine the origin of the pituitary lesion, for which the guidelines shown in Fig. 1C can be followed.

### Characterisation of the lesion

To characterise the lesions, at least the morphological sequences enhanced on T1 and T2 are required. The signal characteristics will be described in the different enhancements of the pituitary lesion compared with the healthy gland or the adjacent temporal lobe. These characteristics allow a certain approximation to the histological/tissue characterisation of the lesions to differentiate solid lesions

from cystic and mixed lesions while also attempting to know the content of cystic lesions (protein, haemorrhagic, cholesterol, etc.). In this sense, contrast uptake is also used for characterisation.

Dynamic T1 imaging, or dynamic contrast-enhanced MR imaging (DCE-MRI), is used to assess vascularisation and the degree of tissue permeability. In pituitary disease, it has been used to differentiate normal pituitary tissue from pituitary adenomas. As pituitary tissue is more vascularised than adenomas, normal pituitary tissue uptake curves over time show a higher and faster enhancement peak with a steeper slope than adenomas<sup>37</sup> (Table 1).

Including coronal sequences on T2 can help identify microprolactinomas (hyperintense on T2), avoiding the use of contrast. Also, silent corticotroph adenomas may have

**Table 2** Basic content of a pituitary MRI report.

Symptoms and signs and initial diagnostic suspicion <sup>a</sup> :	
<b>Type of study and previous treatment (if applicable)<sup>a</sup></b>	
<input type="checkbox"/> First diagnostic study	
<input type="checkbox"/> Follow-up study:	Previous treatment:
<b>1. Pituitary lesion or structural alteration</b>	
<input type="checkbox"/> Pituitary lesion	<input type="checkbox"/> Structural alteration
<b>2. Origin of the lesion</b>	
<input type="checkbox"/> Hypothalamus	<input type="checkbox"/> Ectopic neurohypophysis
<input type="checkbox"/> Optic chiasm	<input type="checkbox"/> Stalk alteration:
<input type="checkbox"/> Pituitary stalk	<input type="checkbox"/> thickening
<input type="checkbox"/> Cavernous sinus	<input type="checkbox"/> V-shaped
	<input type="checkbox"/> A-shaped
<input type="checkbox"/> Pituitary gland	<input type="checkbox"/> Alteration of adenohypophysis
<input type="checkbox"/> Meninges	<input type="checkbox"/> Alteration of neurohypophysis signal
<input type="checkbox"/> Sphenoid sinus	
<input type="checkbox"/> Bone	<input type="checkbox"/> Empty sella turcica
<b>3. Characterisation of the lesion signal, including on T2 with respect to the temporal lobe</b>	
<b>4. Lesion size<sup>b</sup></b>	
$Vol = \frac{A \times B \times C}{2}$ (anteroposterior (A), craniocaudal (B) and anterolateral (C) axes)	
<b>5. Lesion extension and relationship with neighbouring structures</b>	
Suprasellar extension and relationship with chiasm	
Posterior extension with analysis of the clivus	
Extension to sphenoid sinus <sup>c</sup>	<input type="checkbox"/> Grade 0 <input type="checkbox"/> Grade 1 <input type="checkbox"/> Grade 2 <input type="checkbox"/> Grade 3 <input type="checkbox"/> Grade 4
Invasion of cavernous sinuses <sup>d</sup>	<input type="checkbox"/> Grade 0 <input type="checkbox"/> Grade 1 <input type="checkbox"/> Grade 2 <input type="checkbox"/> Grade 3A <input type="checkbox"/> Grade 3B <input type="checkbox"/> Grade 4
<b>6. Description or additional features</b>	
<b>7. Comparison with previous studies (if applicable)</b>	
<b>8. MOST LIKELY RADIOLOGICAL DIAGNOSIS</b>	

<sup>a</sup> Minimum information<sup>97</sup> that the clinician must provide in the test request.

<sup>b</sup> Chuang et al.<sup>38</sup>.

<sup>c</sup> Classification of Hardy et al.<sup>45</sup>.

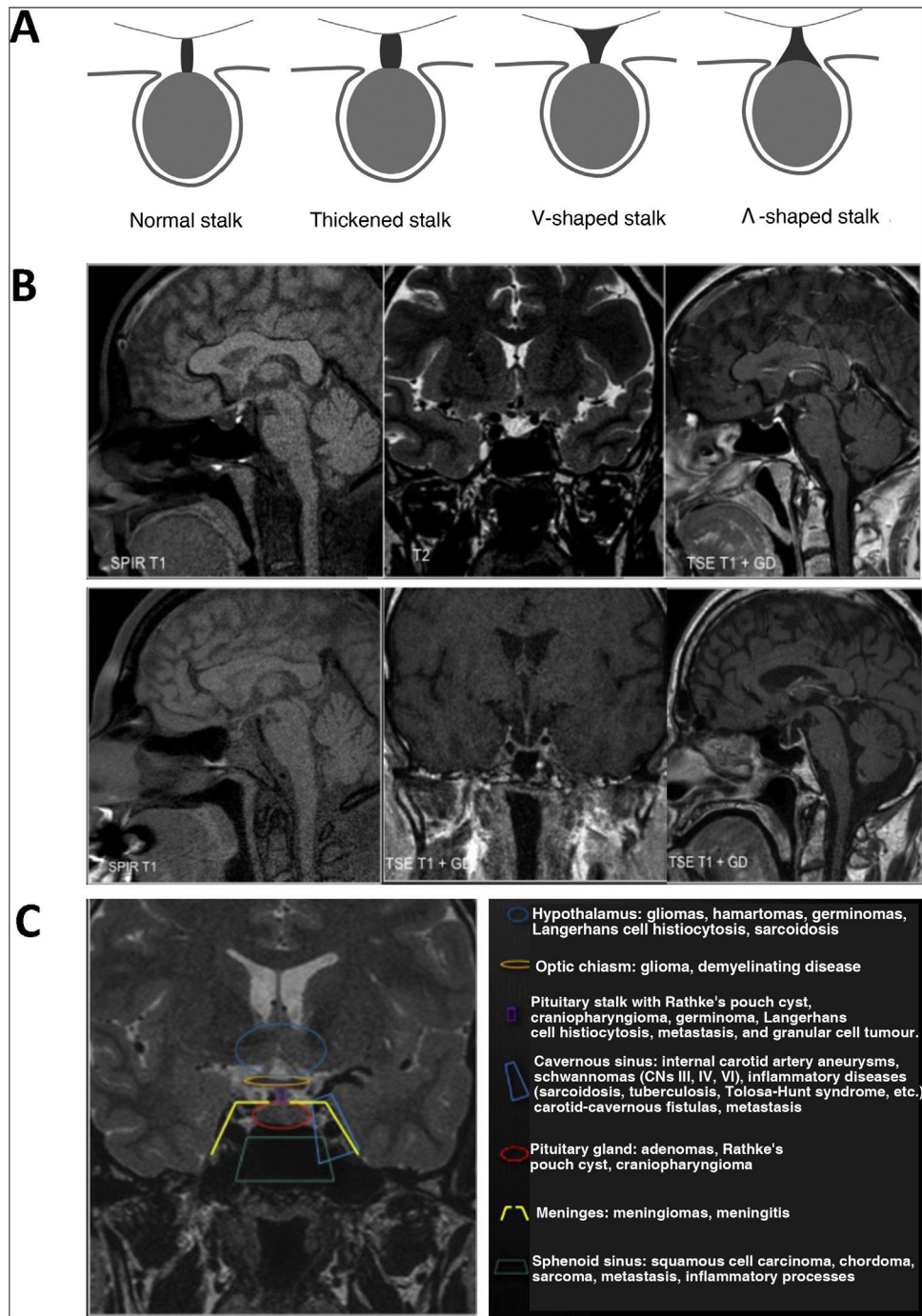
<sup>d</sup> Knosp grades. Micko et al.<sup>47</sup>.

a microcystic pattern on T2 and their identification is important because they are more aggressive. Finally, in acromegaly, it offers information to predict the response to analogues<sup>33</sup>.

### Size of the lesion

The size must be defined by measuring the three axes of the space (anteroposterior [A], craniocaudal [B] and transverse




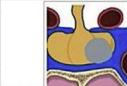




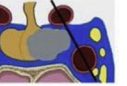
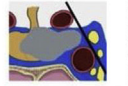
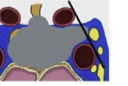




**Figure 1** Morphological alterations. A) Stalk morphologies. B) Upper panels: ectopic neurohypophysis and hypoplasia of the stalk and adenohypophysis; lower left panel: diabetes insipidus (absence of normal hypersignal on T1 of the neurohypophysis). Lower centre and right panels: empty sella turcica (coronal and sagittal section). C) Classification of sellar and parasellar lesions according to their origin.

[C]), and this information at least must be included in the report. The geometric formula can be used to calculate the volume  $Vol = \frac{A \times B \times C}{2}$ , with the limitation that we assume the lesion to be spherical<sup>38</sup>. A 3D volumetric analysis can also be carried out with specific software, and although it is a more laborious option, it allows a better definition of irregular or lobulated adenomas. However, although this last approach

is more accurate and would be of special interest in post-surgical follow-up, it is not yet routinely applied in clinical practice and is used more in research studies. Both methods have been compared<sup>38</sup> and are limited by the intra- and interobserver variability in the delimitation of the lesions, especially when the difference in intensity of the adenomas concerning the normal parenchyma is scarce.

**Table 3** Extension and relationship with neighbouring structures.

Extension and relationship with neighbouring structures					
<b>Suprasellar extension and relationship with chiasm</b>		Visual symptoms (hemianopia or bitemporal quadrantanopia) are related to optic chiasm compression. The distance to the chiasm must be defined, and if it makes contact with, compresses or displaces it.			
<b>Posterior extension with analysis of the clivus</b>					
<b>Extension to sphenoid sinus</b>		It is evaluated according to the Hardy grades, considering grades 3 and 4 invasive. Images by Serioli et al.97 (CC 4.0 licence)			
<b>Sellar enlargement</b>			<b>Sellar erosion</b>		
					
Grade 0: intact with normal contour	Grade 1: intact with bulging floor	Grade 2: intact with enlarged fossa	Grade 3: localised sellar destruction	Grade 4: diffuse destruction	
<b>Invasion of cavernous sinuses</b>					
It is described according to the Knosp classification, considering grades 3 and 4 to be invasive. Images by Serioli et al.97 (CC 4.0 licence)					
					
Grade 0: The tumour does not invade the cavernous sinus. All intracavernous anatomical structures are preserved. The tumour does not exceed the tangential line that joins the medial wall of the supracavernous internal carotid artery with the intracavernous internal carotid artery.	Grade 1: The tumour exceeds the medial tangent, which joins the two medial borders of the supra- and intracavernous carotid, but does not exceed the tangential line that joins the two centres of both carotids. The superior and inferior venous compartments may be obstructed, depending on whether the lesion grows superiorly or inferiorly, respectively.	Grade 2: The tumour extends outside the intercarotid line without exceeding the lateral tangent of the intra- and supracavernous carotid artery.	Grade 3A: The tumour extends laterally to the lateral tangential line that joins the supracavernous carotid portion with the intracavernous portion. In the superior compartment. This grade has a lower growth rate than grades 3B, or 4.	Grade 3B: The tumour extends laterally to the lateral tangential line that joins the supracavernous carotid portion with the intracavernous portion in the inferior compartment.	Grade 4: The carotid artery is entirely enclosed by the tumour, with all the venous compartments obliterated.

In addition, it is important always to use the same volume calculation method to estimate evolutionary changes correctly.

### Extension and relationship with neighbouring structures

The report must describe the extent of the injury and its relationship with neighbouring structures, considering the established classifications summarised in [Table 3](#).

### Comparison with previous MRI studies

If it is not the first diagnostic study, the study should be obtained using the same protocol and configuration as the original or the previous ones<sup>19</sup>. Ideally, it will be performed on the same MRI equipment, with the images stored in the centre's picture archiving and communication system (PACS). The report should compare previous studies and put the current study in context<sup>19,21,39</sup>.

- Clinical context of the case: initial diagnosis and treatment performed.
- Comparison with previous radiological studies, both with the diagnostic and follow-up studies.
- If surgery has been carried out, consider the changes inherent to the intervention, both in the immediate post-operative period and in subsequent monitoring.
- Identify possible tumour remnants or recurrence (tissue that behaves like the initial lesion in the diagnostic study).
- Describe possible complications: cerebrospinal fluid leaks, haemorrhages, etc.

### Additional tests and staging of aggressive PitNETs

If an aggressive PitNET is suspected, a correct staging of the disease should be performed. It is necessary to investigate the possible presence of metastases when faced with data such as accelerated growth, invasive tumour, and growth despite adequate treatment and lack of consistency between symptoms, biochemical data and radiological findings<sup>40</sup>. The main locations of metastases are the spinal cord, cervical lymph node chains and, less frequently, the liver, bone and lung. For this study, the imaging options are full-body PET and CT. FDG-PET has greater sensitivity in staging various oncological processes compared to full-body CT. Aggressive PitNETs have high avidity for FDG, so they should be considered an imaging technique for remote disease screening. In the case of confirmed metastases, PET with <sup>68</sup>Ga-DOTATATE can be useful to assess the expressivity of somatostatin receptors<sup>41</sup> and to evaluate alternative treatment with analogues labelled with <sup>177</sup>Lu<sup>42</sup>.

### Imaging tests in the surgical planning for PitNETs

#### Presurgical evaluation

In this context, the purposes of the neuroradiological study of pituitary adenomas are those already described: to identify the lesion and define the tumour's spatial relationships with the surrounding structures. Among these, the following stand out: the effect on the optic nerves/chiasm, the extension in the cavernous sinuses and its relationship with the adjacent internal carotid artery, the parasellar extension and the invasion of the base of the skull/foramina ovale, clinoid process, planum sphenoidale, clivus and sphenoid

sinuses. In addition to the basic MRI study described above (Table 2), it is useful to have complementary sequences such as MR angiography<sup>43,44</sup>, especially when suspecting a possible vascular nature of the sellar lesion or stenosis of the adjacent internal carotid artery.

#### MRI data for surgical planning for microadenomas

Pituitary microadenomas are the most common intrasellar neoplasms, and their diagnosis is based on the presence of indirect and direct findings. The indirect findings are: a) lateral displacement of the pituitary stalk; b) morphological alteration of the upper contour (sellar diaphragm), and c) irregularity or focal convexity of the sellar floor. The direct findings identify round or oval lesions, with a different signal from the rest of the glandular parenchyma in baseline sequences or with less contrast uptake, compared to the rest of the adenohypophysis. Microadenomas may show hyperintensity on T1-weighted images due to increased protein content or haemorrhage from part or all of the lesion.

In the case of microadenomas, it is important to determine the lateralisation, that is, the precise location in one of the two halves of the anterior lobe, if the aim is to preserve the healthy pituitary half to maintain functionality.

#### MRI data for surgical planning for macroadenomas

Pituitary macroadenomas usually extend outside the sella turcica. For planning, it is necessary to clarify the structure of the lesion, its consistency (firm, cystic, necrotic or haemorrhagic) and its relation with the surrounding anatomical structures. The tumour usually extends cranially, tending to compress the optic chiasm; it may remain subdiaphragmatic or rupture the sellar diaphragm. The position of the adenoma should be described when it extends into the suprasellar region. The adenoma may extend downward into the sphenoid sinus or laterally into the cavernous sinus<sup>45</sup>. It is of utmost importance to assess whether the cavernous sinus is compressed or invaded (Table 3) or if there is an invasion of the third ventricle and to plan the approach (either transsphenoidal or transcranial). Likewise, the neurosurgeon needs to know a priori if there is an invasion of the adventitia of the adjacent internal carotid artery because, in this case, if the resection is aggressive, it can tear the carotid artery and cause massive arterial bleeding.

One common way to approach it surgically is by nasal endoscopy. Therefore, it is convenient to describe the position according to four regions established by two virtual planes: one passes through the inferior surface of the chiasm and the mammillary bodies and the other through the posterior margin of the chiasm and the dorsum sellae. The resulting regions are the suprachiasmatic, the subchiasmatic, the retrosellar and the ventricular.

#### Usefulness of CT in surgical planning

In selected cases, CT will provide more detail about the presence of calcified components of the lesion and achieve a precise definition of the bone boundaries. If the surgical approach chosen is the transsphenoidal one, the CT will offer relevant information on the degree of pneumatization of the sphenoid sinus; if it is transcranial (e.g. supraorbital), we will obtain information on the degree of pneumatization of the frontal sinus. In addition, CT allows a detailed

overview of the bone map of the nasal passages, paranasal sinuses and skull base. It allows the study of the anatomical landmarks referenced in nasosinusal endoscopic surgery (nasal turbinates, uncinata processes, etc.) and the degree of pneumatization and integrity and positioning of the bony walls of the sphenoid and frontal sinuses.

#### Prediction of post-surgical remission

The key factor for predicting postoperative remission is the degree of invasion of the cavernous sinus<sup>46,47</sup>. The importance of the differentiation between grades 3A and 3B within Knosp grade 3 (Table 3) in predicting the success of surgery has recently been described, being significantly less in grade 3B<sup>47-49</sup>. With this objective of predicting post-surgical remission and recurrence, diffusion-weighted imaging (DWI) sequences and the apparent diffusion coefficient (ADC) could be useful<sup>50</sup>.

#### Intraoperative assessment by MRI

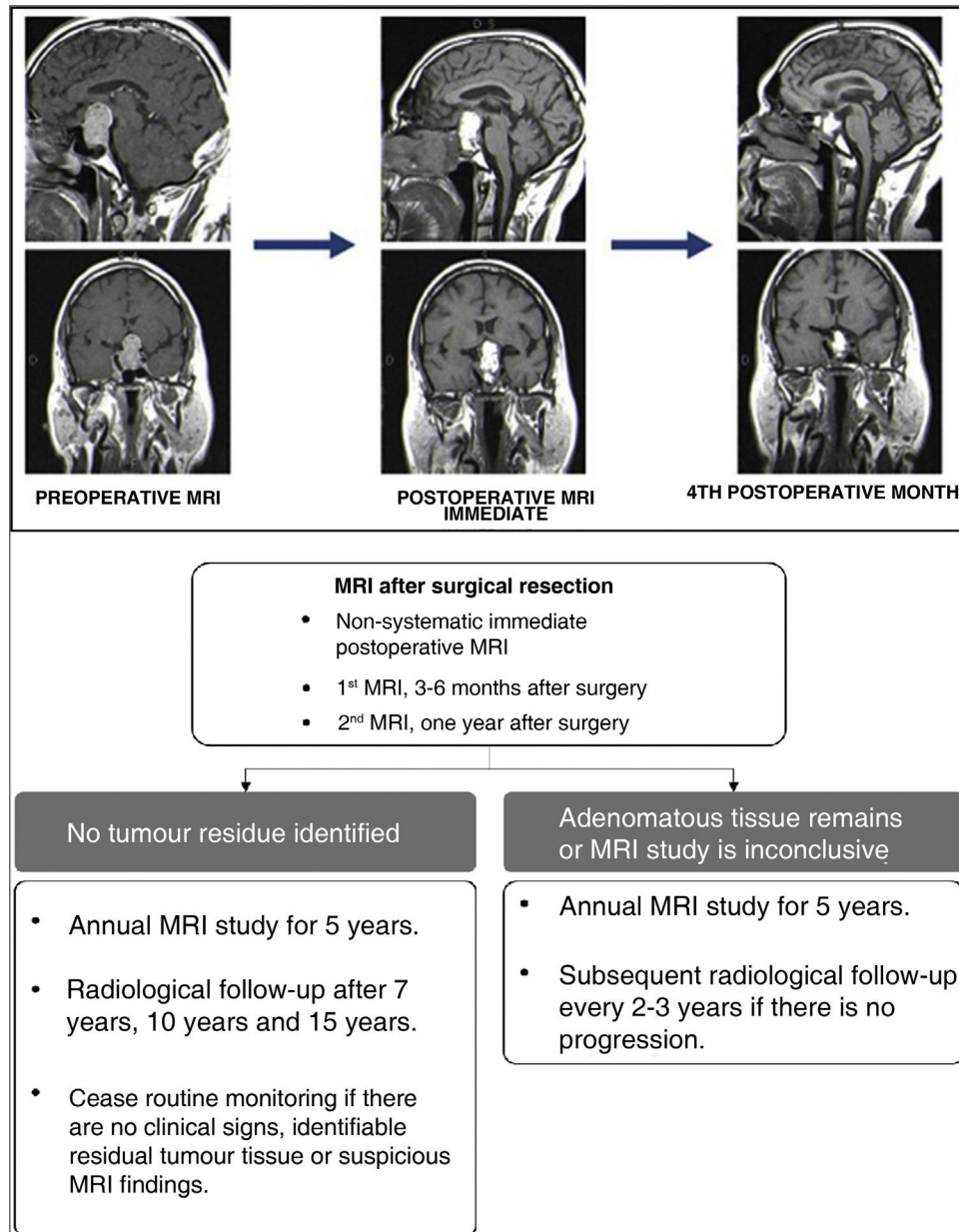
The use of intraoperative MRI (iMRI) has been described since 1994<sup>51</sup>. However, its implementation in clinical practice is still very low, and the literature on the matter is controversial. In a recent review<sup>52</sup> on iMRI modalities (low field, high field and neuronavigation), advantages are cited, such as better visualisation of the cavernous sinus, real-time information for the surgeon, and therefore the possibility of increasing the rate of complete tumour resection and preservation of healthy gland, among other things. On the other hand, the disadvantages are the duration of the surgery and the increase in costs.

#### Post-surgical evaluation by MRI

There is no consensus regarding the optimal time to perform the post-surgical MRI study<sup>53,54</sup>. Immediate post-surgical MRI (within the first week after surgery) detect tumour remnants during evolutionary follow-up, serving as the basis for subsequent follow-up MRI scans<sup>55-57</sup>. It is useful to diagnose possible complications and to assess the normal gland and the degree of resection of the lesion<sup>21,58</sup> (Fig. 2, upper panel). The following can be taken into account for reference:

- If the signal intensity and contrast uptake are similar to those of the lesion in the pre-surgical study, said tissue is suspected of being a tumour remnant.
- When contrast enhancement is linear and peripheral, it is more likely to correspond to post-surgical changes<sup>59</sup>. Knowledge of the radiological characteristics of the materials implanted in the sellar region is also very important. Some materials, such as fat, can be identified up to years after surgery, whereas others, such as haemostatic materials, only be for a few weeks after surgery. On the other hand, it is important to bear in mind that the disposition and characteristics of the fat used to cover the surgical defect of transsphenoidal surgery vary between the study immediately after surgery and the subsequent follow-up studies.
- In the dynamic study, identifying the suspected tumour remnant with an uptake thickness >3.9 mm is related to





**Figure 2** Upper: evolution of pituitary adenoma four months after surgery. Lower: radiological follow-up with MRI for non-functioning PitNETs.

Translated and adapted from Cortet-Rudelli et al.<sup>55</sup>, 2015.

tumour remnants with a sensitivity of 89% and specificity of 97%<sup>60</sup>.

#### Radiological follow-up of non-functioning PitNETs

In late postoperative follow-up, and especially in non-functioning PitNETs, MRI is usually performed between the third and sixth month after the intervention<sup>21,55</sup>. Although in the immediate post-surgical follow-up scan, it is possible to get an indication of whether partial or complete resection has been achieved, it is not until 4–6 months after surgery that the materials of the surgical site are reabsorbed and that the degree of tumour resection can be clearly assessed. In functioning PitNETs, routine radiological follow-up is unnecessary if hormonal remission is confirmed

and complications or recurrence are not suspected. Fig. 2 (lower panel) outlines a post-surgical follow-up protocol for non-functioning PitNETs. The existence of tumour remnants after surgery, especially invading the cavernous sinuses, is the factor that most defines the risk of recurrence, and, after analysing the different series, it is estimated that this recurrence appears in 47% of cases if there are remnants vs 15% if they are none<sup>55</sup>. The variables related to a lower recurrence rate are older age and a greater extent of tumour resection<sup>61</sup>.

There are no specific recurrence markers in non-functioning PitNETs. Some 85% of recurrences usually occur in the first five years. Among patients not treated with radiotherapy, 20% present recurrence before five years and more

than 50% after 10 years<sup>62</sup>. Late recurrences are also common, so long-term follow-up with MR imaging should be performed at least until other reliable methods that predict tumour recurrence have been identified<sup>62</sup>.

## Imaging tests in planning radiotherapy treatment

Volumetric T1-weighted sequences with contrast provide precision when outlining the adenomas and the risk organs surrounding them, mainly the chiasm and the optic nerves. In radiotherapy and after surgery that requires abdominal fat grafting, fat suppression sequences can be useful for defining residual adenoma<sup>56,63</sup>. Reconstructions must be obtained in the axial plane since most radiotherapy planners only use this plane to be able to make a rigid or deformable registration between the planning MRI and the planning CT. The latter will be required in most cases (except Gamma Knife or MR-Linac units) for dose calculation. In patients who cannot undergo an MRI, a CT with slice reconstruction every 1–2 mm and adding iodinated contrast is the test of choice<sup>56</sup>.

Currently, the use of metabolic imaging in planning radiotherapy for treating pituitary adenoma is experimental, with various techniques under study<sup>57,64–66</sup>.

## Usefulness of MRI in the prognosis of PitNETs and monitoring of response to treatment

### MRI in the prognosis

The depth of invasion is a marker of aggressiveness of a PitNET. However, to be considered an aggressive adenoma, it must also present an early recurrence (6–12 months after surgery), rapid tumour growth, and resistance to conventional treatment<sup>40,67</sup>. In any case, the definition of an aggressive PitNET is achieved in combination with the histopathological diagnosis using proliferation indicators<sup>67</sup> and theragnostics<sup>68</sup>.

Most studies that relate the radiological aspect and the histological and molecular characteristics of aggressiveness have been done concerning acromegaly<sup>69–74</sup>. According to these relationships, different subtypes of GH-producing PitNETs have been described<sup>70</sup>. In this pathology, signal hypointensity on T2 has been related to other tumour characteristics, histological (densely granulated pattern) and clinical (such as better response to somatostatin analogues [SSA]) and, therefore, with its prognosis<sup>69,71–73</sup>. Expression of somatostatin receptor 3 (SSTR3) and dopamine D5 receptor (DRD5) are associated with extrasellar or suprasellar extension. In addition, the expression of DRD5 is greater in hyperintense adenomas on T2, and its expression is directly related to Knosp grades and tumour diameter<sup>69</sup>. On the other hand, the absence of the normal hypersignal on T1 of the neurohypophysis in the pre-surgical MRI is a predictor of post-surgical diabetes insipidus<sup>74</sup>.

In a recent meta-analysis that included tumours of various strains, of which 9.5% were neuroendocrine and 2% pituitary, ADC was related to the degree of cell proliferation and histopathological characteristics such as the

expression of different receptors, nuclear polymorphism and proliferation potential (especially MIB-1, Ki67), which would help plan the surgical approach and predict the tumour behaviour<sup>75</sup>. A strong correlation between low ADC values and MIB-1 (Ki67) has been described, demonstrating the potential of diffusion imaging as a biomarker of what was previously known as atypical and proliferative adenomas<sup>76</sup>.

### Morphological criteria to determine the response to radiotherapy treatment

The parameter that has traditionally provided information on the response to treatment is the size of the lesion<sup>77</sup>. Since these are slow-growing tumours, a reduction and even stability in size have been considered favourable responses. For this reason, it is important that, in addition to the tumour characteristics, the reduction, stability or increase in volume is also registered. When the patient has received radiotherapy treatment, the increase in signal on T2-weighted imaging is considered a criterion of favourable response to treatment. On the other hand, the loss of signal on T2 (hyposignal) in the follow-up of adenomas should be evaluated with caution, since it may reflect a transformation to a more fibrous or more cellular tumour (malignant degeneration)<sup>77</sup>.

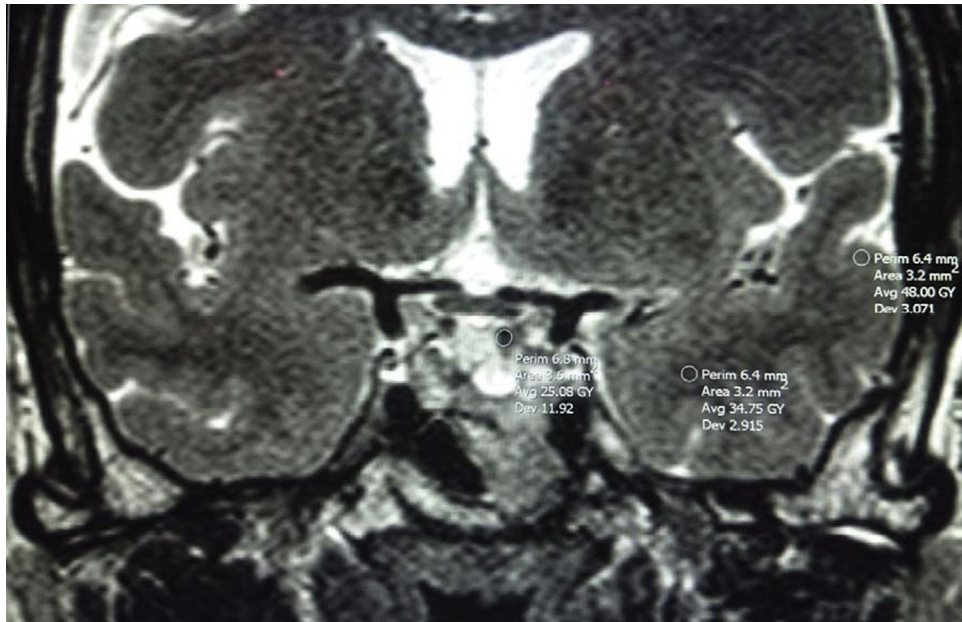
In adenomas larger than 3 cm, the measurements' differences before and after radiotherapy have been evaluated by calculating the volume using the three diameters. The results support performing 3D volumetric analysis, instead of 2D, for the measurement of large or giant adenomas<sup>78</sup>. 3D volumetry is more sensitive to changes in size, but obtaining it is more complex<sup>79</sup>.

### Prediction of response to SSA treatment in acromegaly

The hypointensity of PitNETs on T2-weighted sequences has been associated with the presence of a densely granulated pattern<sup>80</sup>, as well as with a significantly better response to SSA after surgery<sup>73</sup>. Furthermore, the reduction in GH with treatment is also significantly greater<sup>81–83</sup>, with a greater reduction in GH production and tumour size the greater the hypointensity detected<sup>84</sup>. Hypointensity on T2 also correlates with a greater reduction in GH after an octreotide test and a smaller size and invasiveness at diagnosis<sup>82,84</sup>. However, the reason for the better response to SSA in hypointense adenomas is unknown<sup>33</sup>.

It is therefore important to establish how to define the intensity on T2 and it can be done in two ways.

- Comparing it with the healthy pituitary gland, provided that it can be well discriminated<sup>84</sup>.
- Or comparing it with the adjacent temporal lobe (cerebral white and grey matter [Fig. 3])<sup>78,80,84</sup>. It will be hypointense when the MRI signal is equal to or less than that of the white matter and less than that of the grey matter, hyperintense when the signal is equal to or greater than that of the grey matter, and isointense when the signal is between those of the white and grey matter. Potorac et al.<sup>84</sup> propose that since the characteristics of iso- and hyperintense are similar, they could be grouped



**Figure 3** Measurement of the region of interest (ROI) in the solid portion of the adenoma, white matter and grey matter of the temporal lobe. In this case, it would be a hypointense pituitary NET on T2. Avg: average; Dev: standard deviation; Perim: perimeter.

into two categories: hypointense and non-hypointense (iso- and hyperintense).

- It could be a qualitative or quantitative comparison (using the measurements of the region of interest (ROI) of the PitNET, white and grey matter [Fig. 3]). Methodologically, a good correlation between the use of ROI and direct visual assessment has been described<sup>33,84</sup>.

Another radiological parameter is the homogeneity/heterogeneity of the tumour. More homogeneous adenomas have higher GH levels at diagnosis, but this does not correlate with reduced GH or the volume or invasiveness of the adenoma<sup>82,83</sup>.

### Prediction of response to treatment with dopamine agonists (DAs) in acromegaly

Although DAs are indicated in cases with slightly elevated IGF-1<sup>85</sup>, there is no evidence in the literature that the intensity on T2 can predict the response to DAs. However, it is suggested that DAs would be the treatment to consider in the case of poorly granulated tumours, with little expression of SSTR2 and hyperintense on T2 with slightly elevated IGF-1<sup>85</sup>.

### Prediction of response to DA treatment in prolactinomas

Prolactinomas are usually hypointense and occasionally isointense on T1 but rarely hyperintense (haemorrhage or protein content). On T2, 80% of prolactinomas are hyperintense, although with differences according to sex. Heterogeneity on T2 is more common in men with areas of focal necrosis or old haemorrhage, and heterogeneity

is associated with poorer response to DAs. In young men, prolactinomas are usually larger and more invasive, have higher PRL levels and have a worse response to DAs than homogeneous adenomas<sup>86</sup>.

Adenomas hypointense on T2 are also more common in men, possibly due to the deposition of amyloid material in these tumours<sup>87–89</sup>. It has been suggested that hypointensity on T2 would be related to resistance to DAs, although the evidence is controversial<sup>86–88,90</sup>.

Regarding the response to treatment with cabergoline, it is essential to standardise the report, stating whether there is a volumetric reduction of the prolactinoma at three months as a criterion of good long-term response<sup>91</sup>.

It has been described that early changes in intensity on T2 after treatment with cabergoline can predict a favourable response regarding regression and the almost total disappearance of the tumour<sup>92</sup>.

Cystic prolactinomas, more common in women, secrete less PRL<sup>86</sup> and have traditionally been considered to be resistant. However, it has been shown that they can be treated effectively with DAs, normalising PRL in 18/22 cases and a mean volume reduction of 83.5% in 20/22 cases<sup>93</sup>.

Once controlled PRL levels have been achieved, routine follow-up with MRI is unnecessary<sup>94,95</sup>.

## Future perspectives in pituitary imaging tests

### New MRI techniques

In addition to MR angiography, a sequence already implemented in practice for surgical planning, other sequences with potential utility in studying PitNETs have been investigated. Table 4 summarises the experimental and potential use of said sequences.

**Table 4** MRI sequences that have been applied in the investigation of pituitary disorders.

MRI sequence	Characteristics	Possible applications
Magnetic resonance angiography	Provides detailed images of the arterial system	Detection of intrasellar aneurysms <sup>43</sup> Delimitation of cranial nerves in their cavernous sinus segment <sup>44</sup>
3D-GRE/3D-MPGRE	Higher contrast resolution and they are an alternative or an added value to the dynamic study. Volumetric acquisition with 1 mm voxel	Detection of the smallest microadenomas not visible on conventional imaging <sup>98–100</sup>
FLAIR	An inversion recovery sequence with a long inversion time that removes the signal from the CSF which is, therefore, darker rather than brighter as would usually be seen on T2 sequences	In Cushing's disease, contrast withdrawal delay of a corticotrophic microadenoma can be detected as FLAIR hyperintensity <sup>101</sup>
DWI	Measures the diffusion of water molecules in biological tissues; most commonly used to detect cytotoxic oedema in the setting of acute cerebral ischaemia/infarction	Detection of pituitary apoplexy/acute pituitary infarction <sup>102</sup> To distinguish intrasellar/suprasellar cystic lesions <sup>103</sup> To distinguish between adenoma and craniopharyngioma <sup>104</sup> To obtain consistency information for surgical planning <sup>105,106</sup>
Diffusion tensor	An extension of DWI that analyses the directional diffusion of water molecules in biological tissue	Tractography of the optic nerve for surgical planning and predicting the probability of visual recovery after transsphenoidal surgery <sup>107–109</sup>
Apparent diffusion coefficient	A subtype of DWI	Its usefulness in predicting tumour consistency for surgical planning is still debatable <sup>110–117</sup> Assessment of aggressiveness by determining tumour heterogeneity (recurrence and proliferative potential) <sup>110</sup> To differentiate persistence vs inflammatory tissue/granulation in adenomas treated with surgery earlier than the morphological image <sup>118</sup>
Weighted perfusion	Evaluates tissue perfusion at the capillary level	Evaluation of vascularisation of the adenoma before surgery <sup>119</sup> Identification of other vascular lesions (e.g. meningioma) that may be confused <sup>120,121</sup>
Magnetic resonance spectroscopy	Provides insight into metabolic function by measuring different metabolites (e.g. N-acetyl aspartate, choline compounds, creatine/phosphocreatine)	Differentiation of adenoma from a normal gland <sup>122</sup> Differential diagnosis of suprasellar lesions <sup>123–126</sup> Prediction of the response of somatotrophic tumours to therapy with somatostatin analogues <sup>127</sup>
Magnetic resonance elastography	Measures shear wave propagation through the tissue of interest to estimate stiffness	Surgical planning estimating whether an adenoma is likely to be soft (and suctionable), intermediate or firm (requiring curettage for resection) <sup>128,129</sup>
Steady-state balanced free precession (e.g. CISS; FIESTA-C)	Image contrast determined by the T2/T1 ratio of the tissue; in practice, very watery (good contrast between CSF and other structures) but also sensitive to post-contrast enhancement	Improved detection of adenoma in Cushing's disease <sup>130</sup> Better assessment of cavernous sinus invasion <sup>130</sup> Prediction of adenoma consistency <sup>131</sup> Improvements in the delineation of the optic nerves and chiasm in large pituitary tumours <sup>132</sup>

3D-GRE/3D-MPGRE: three-dimensional gradient echo sequences/three-dimensional multiplanar gradient echo sequences; DWI: diffusion-weighted imaging; FLAIR: fluid attenuation inversion recovery; CSF: cerebrospinal fluid.

Adapted from Bashari et al.<sup>20</sup>.



## Nuclear medicine merged or co-registered with MRI

One of the advantages of the metabolic study of the pituitary gland is the variable affinity for the different radiotracers. This allows different studies to be combined to evaluate the pituitary gland and guide the clinician in therapeutic decisions. The merging of PET with MRI makes it possible to combine the sensitivity of metabolic tests with the anatomical resolution of MRI in a single study. Still, this equipment is hardly available in normal clinics due to its novelty and price, so the most common is co-registration software.

The combination of FDG and <sup>68</sup>Ga-DOTATE benefits patients with important structural changes after previous interventions<sup>66</sup>. Under normal conditions, the pituitary gland does not show significant avidity for FDG, but pituitary adenomas do, even if they are benign. In the case of DOTATE, both healthy and pathological pituitary tissue show avidity. The combination of the two studies can make it possible to differentiate pituitary adenoma (FDG+/DOTATE+) and normal pituitary tissue (FDG-/DOTATE+)<sup>66</sup>. Although semi-quantitative methods (FDG/DOTATE ratio) can differentiate between healthy and pathological tissue, there are currently no standardised values.

Another useful tracer in the assessment of PitNETs is co-registration with methionine (MET). It makes it possible to differentiate active tumours from fibrosis, bleeding, cysts, etc. In addition, its better tumour-to-brain uptake ratio allows a better delineation of lesions and resolution. It has better sensitivity than FDG for detecting residual tumours, especially in patients with recurrent microadenomas<sup>22</sup>. However, FDG is highly specific; if a study is FDG positive, this patient likely has residual tumour tissue<sup>96</sup>. In cases in which MRI cannot differentiate between tumour and scar tissue, co-registration with these metabolic techniques is very useful. The main limitation of MET is its short half-life, which requires a cyclotron at the centre itself. Tracers with <sup>18</sup>F-methionine are currently being developed, with promising results.

## Funding

The article was financed by the Fundación de la Sociedad Española de Endocrinología y Nutrición (FSEEN) [Foundation of the Spanish Society of Endocrinology and Nutrition] thanks to an unrestricted grant from Pfizer. Pfizer has not participated in the drafting or content of the article. This document has received the endorsement of the SEEN and the Sociedad Española de Neuroradiología (SENR) [Spanish Society of Neuroradiology].

## Conflicts of interest

None of the authors have conflicts of interest with respect to the content of this article.

## Acknowledgements

The authors appreciate the collaboration of Dr Blanca Piedrafita, from Medical Statistics Consulting S.L., in the preparation and editing of the manuscript. All the authors

contributed to the writing, critical review of content and approval of the article's final version.

## References

- Asa SL, Casar-Borota O, Chanson P, Delgrange E, Earls P, Ezzat S, et al. From pituitary adenoma to pituitary neuroendocrine tumor (PitNET): An International Pituitary Pathology Club proposal. *Endocr Relat Cancer*. 2017;24:C5–8, <http://dx.doi.org/10.1530/erc-17-0004>.
- Iglesias P, Arcano K, Trivino V, Garcia-Sancho P, Diez JJ, Villabona C, et al. Prevalence, clinical features, and natural history of incidental clinically non-functioning pituitary adenomas. *Horm Metab Res*. 2017;49:654–9, <http://dx.doi.org/10.1055/s-0043-115645>.
- Tjornstrand A, Gunnarsson K, Evert M, Holmberg E, Ragnarsson O, Rosen T, et al. The incidence rate of pituitary adenomas in western Sweden for the period 2001–2011. *Eur J Endocrinol*. 2014;171:519–26, <http://dx.doi.org/10.1530/eje-14-0144>.
- Asa SL. Tumors of the pituitary gland. In: Rosai J, editor. *Atlas of Tumor Pathology (AFIP) third series*. Washington, D. C.: Armed Forces Institute of Pathology; 1998.
- Asa SL. Practical pituitary pathology: What does the pathologist need to know? *Arch Pathol Lab Med*. 2008;132:1231–40, [http://dx.doi.org/10.1043/1543-2165\(2008\)132\[1231:pppwwt\]2.0.co;2](http://dx.doi.org/10.1043/1543-2165(2008)132[1231:pppwwt]2.0.co;2).
- Lloyd R, Osamura RY, Klöppel G, Rosai J. In: IARC, editor. *WHO Classification of Tumours of Endocrine Organs*. Geneva: World Health Organization; 2017.
- Saeger W, Lüdecke DK, Buchfelder M, Fahlbusch R, Quabbe HJ, Petersenn S. Pathohistological classification of pituitary tumors: 10 years of experience with the German Pituitary Tumor Registry. *Eur J Endocrinol*. 2007;156:203–16, <http://dx.doi.org/10.1530/eje.1.02326>.
- Raverot G, Burman P, McCormack A, Heaney A, Petersenn S, Popovic V, et al. European Society of Endocrinology Clinical Practice Guidelines for the management of aggressive pituitary tumours and carcinomas. *Eur J Endocrinol*. 2018;178:G1–24, <http://dx.doi.org/10.1530/EJE-17-0796>.
- Karavitaki N. Prevalence and incidence of pituitary adenomas. *Ann Endocrinol (Paris)*. 2012;73:79–80, <http://dx.doi.org/10.1016/j.ando.2012.03.039>.
- Fernandez A, Karavitaki N, Wass JA. Prevalence of pituitary adenomas: A community-based, cross-sectional study in Banbury (Oxfordshire, UK). *Clin Endocrinol (Oxf)*. 2010;72:377–82, <http://dx.doi.org/10.1111/j.1365-2265.2009.03667.x>.
- Dekkers OM, Karavitaki N, Pereira AM. The epidemiology of aggressive pituitary tumors (and its challenges). *Rev Endocr Metab Disord*. 2020;21:209–12, <http://dx.doi.org/10.1007/s11154-020-09556-7>.
- Osamura RYGA, Korbonits M, Kovacs K, Lopes MBS, Matsuno A, Trouillas J. Pituitary adenoma. *World Health Organization Classification of Tumours of Endocrine Organs, 2017*. Lyon: IARC; 2017. p. 14–8.
- Guaraldi F, Zoli M, Righi A, Gibertoni D, Marino Picciola V, Faustini-Fustini M, et al. A practical algorithm to predict postsurgical recurrence and progression of pituitary neuroendocrine tumours (PitNET)s. *Clin Endocrinol (Oxf)*. 2020;93:36–43, <http://dx.doi.org/10.1111/cen.14197>.
- Villa C, Vasiljevic A, Jaffrain-Rea ML, Anserge O, Asioli S, Barresi V, et al. A standardised diagnostic approach to pituitary neuroendocrine tumours (PitNETs): A European Pituitary Pathology Group (EPPG) proposal. *Virchows Arch*. 2019;475:687–92, <http://dx.doi.org/10.1007/s00428-019-02655-0>.
- Picó A, Aranda-López I, Sesmiolo G, Toldos-González Ó, Japón MA, Luque RM, et al. Recommendations on the pathological

- report of pituitary tumors. A consensus of experts of the Spanish Society of Endocrinology and Nutrition and the Spanish Society of Pathology. *Endocrinol Diabetes Nutr.* 2021;68:196–207, <http://dx.doi.org/10.1016/j.endinu.2020.10.004>.
16. Drummond J, Roncaroli F, Grossman AB, Korbonits M. Clinical and pathological aspects of silent pituitary adenomas. *J Clin Endocrinol Metab.* 2019;104:2473–89, <http://dx.doi.org/10.1210/jc.2018-00688>.
  17. Mete O, Gomez-Hernandez K, Kucharczyk W, Ridout R, Zadeh G, Gentili F, et al. Silent subtype 3 pituitary adenomas are not always silent and represent poorly differentiated monomorphous plurihormonal Pit-1 lineage adenomas. *Mod Pathol.* 2016;29:131–42, <http://dx.doi.org/10.1038/modpathol.2015.151>.
  18. Nishioka H, Inoshita N, Mete O, Asa SL, Hayashi K, Takeshita A, et al. The complementary role of transcription factors in the accurate diagnosis of clinically nonfunctioning pituitary adenomas. *Endocr Pathol.* 2015;26:349–55, <http://dx.doi.org/10.1007/s12022-015-9398-z>.
  19. Bonneville JF. Magnetic resonance imaging of pituitary tumors. *Front Horm Res.* 2016;45:97–120, <http://dx.doi.org/10.1159/000442327>.
  20. Bashari WA, Senanayake R, Fernández-Pombo A, Gillett D, Koulouri O, Powlson AS, et al. Modern imaging of pituitary adenomas. *Best Pract Res Clin Endocrinol Metab.* 2019;33:101278, <http://dx.doi.org/10.1016/j.beem.2019.05.002>.
  21. Raverot G, Assié G, Cotton F, Cogne M, Boulin A, Dherbomez M, et al. Biological and radiological exploration and management of non-functioning pituitary adenoma. *Ann Endocrinol (Paris).* 2015;76:201–9, <http://dx.doi.org/10.1016/j.ando.2015.04.005>.
  22. Feng Z, He D, Mao Z, Wang Z, Zhu Y, Zhang X, et al. Utility of 11C-methionine and 18F-FDG PET/CT in patients with functioning pituitary adenomas. *Clin Nucl Med.* 2016;41:e130–4, <http://dx.doi.org/10.1097/RLU.0000000000001085>.
  23. Koulouri O, Hoole AC, English P, Allinson K, Antoun N, Cheow H, et al. Localisation of an occult thyrotropinoma with (11)C-methionine PET-CT before and after somatostatin analogue therapy. *Lancet Diabetes Endocrinol.* 2016;4:1050, [http://dx.doi.org/10.1016/S2213-8587\(16\)30311-4](http://dx.doi.org/10.1016/S2213-8587(16)30311-4).
  24. Koulouri O, Steuwe A, Gillett D, Hoole AC, Powlson AS, Donnelly NA, et al. A role for 11C-methionine PET imaging in ACTH-dependent Cushing's syndrome. *Eur J Endocrinol.* 2015;173:M107–20, <http://dx.doi.org/10.1530/EJE-15-0616>.
  25. Tang BN, Levivier M, Heures M, Wikler D, Massager N, Devriendt D, et al. 11C-methionine PET for the diagnosis and management of recurrent pituitary adenomas. *Eur J Nucl Med Mol Imaging.* 2006;33:169–78, <http://dx.doi.org/10.1007/s00259-005-1882-0>.
  26. Nieman LK, Biller BM, Findling JW, Murad MH, Newell-Price J, Savage MO, et al. Treatment of Cushing's Syndrome: An Endocrine Society Clinical Practice Guideline. *J Clin Endocrinol Metab.* 2015;100:2807–31, <http://dx.doi.org/10.1210/jc.2015-1818>.
  27. Nieman LK, Biller BM, Findling JW, Newell-Price J, Savage MO, Stewart PM, et al. The diagnosis of Cushing's syndrome: an Endocrine Society Clinical Practice Guideline. *J Clin Endocrinol Metab.* 2008;93:1526–40, <http://dx.doi.org/10.1210/jc.2008-0125>.
  28. Bonelli FS, Huston IIIJ, Carpenter PC, Erickson D, Young WF Jr, Meyer FB. Adrenocorticotropic hormone-dependent Cushing's Syndrome: Sensitivity and specificity of inferior petrosal sinus sampling. *Am J Neuroradiol.* 2000;21:690–6.
  29. Pinker K, Ba-Ssalamah A, Wolfsberger S, Mlynarik V, Knosp E, Trattnig S. The value of high-field MRI (3T) in the assessment of sellar lesions. *Eur J Radiol.* 2005;54:327–34, <http://dx.doi.org/10.1016/j.ejrad.2004.08.006>.
  30. Satogami N, Miki Y, Koyama T, Kataoka M, Togashi K. Normal pituitary stalk: high-resolution MR imaging at 3T. *AJNR Am J Neuroradiol.* 2010;31:355–9, <http://dx.doi.org/10.3174/ajnr.A1836>.
  31. European Medicines Agency. EMA's final opinion confirms restrictions on use of linear gadolinium agents in body scans 2017. Available from: [https://www.ema.europa.eu/en/documents/referral/gadolinium-article-31-referral-prac-confirms-restrictions-use-linear-gadolinium-agents\\_en.pdfhttps://www.ema.europa.eu/en/news/emas-final-opinion-confirms-restrictions-use-linear-gadolinium-agents-body-scans](https://www.ema.europa.eu/en/documents/referral/gadolinium-article-31-referral-prac-confirms-restrictions-use-linear-gadolinium-agents_en.pdfhttps://www.ema.europa.eu/en/news/emas-final-opinion-confirms-restrictions-use-linear-gadolinium-agents-body-scans).
  32. Nachtigall LB, Karavitaki N, Kiseljak-Vassiliades K, Ghalib L, Fukuoka H, Syro LV, et al. Physicians' awareness of gadolinium retention and MRI timing practices in the longitudinal management of pituitary tumors: a Pituitary Society survey. *Pituitary.* 2019;22:37–45, <http://dx.doi.org/10.1007/s11102-018-0924-0>.
  33. Bonneville JF. A plea for the T2W MR sequence for pituitary imaging. *Pituitary.* 2019;22:195–7, <http://dx.doi.org/10.1007/s11102-018-0928-9>.
  34. Pressman BD. Pituitary imaging. *Endocrinol Metab Clin North Am.* 2017;46:713–40, <http://dx.doi.org/10.1016/j.ecl.2017.04.012>.
  35. Cao J, Lei T, Chen F, Zhang C, Ma C, Huang H. Primary hypothyroidism in a child leads to pituitary hyperplasia: A case report and literature review. *Medicine (Baltimore).* 2018;97:e12703, <http://dx.doi.org/10.1097/md.00000000000012703>.
  36. Turcu AF, Erickson BJ, Lin E, Guadalix S, Schwartz K, Scheithauer BW, et al. Pituitary stalk lesions: The Mayo Clinic experience. *J Clin Endocrinol Metab.* 2013;98:1812–8, <http://dx.doi.org/10.1210/jc.2012-4171>.
  37. Sen R, Sen C, Pack J, Block KT, Golfinos JG, Prabhu V, et al. Role of high-resolution dynamic contrast-enhanced MRI with golden-angle radial sparse parallel reconstruction to identify the normal pituitary gland in patients with macroadenomas. *AJNR Am J Neuroradiol.* 2017;38:1117–21, <http://dx.doi.org/10.3174/ajnr.A5244>.
  38. Chuang C-C, Lin S-Y, Pai P-C, Yan J-L, Toh C-H, Lee S-T, et al. Different volumetric measurement methods for pituitary adenomas and their crucial clinical significance. *Sci Rep.* 2017;7:40792, <http://dx.doi.org/10.1038/srep40792>.
  39. Ouyang T, Rothfus WE, Ng JM, Challinor SM. Imaging of the pituitary. *Radiol Clin North Am.* 2011;49:549–71, <http://dx.doi.org/10.1016/j.rcl.2011.02.012>, vii.
  40. Raverot G. Diagnosis and clinical management of aggressive pituitary tumors. In: Huhtaniemi I, editor. *Encyclopedia of Endocrine Diseases.* Elsevier Science; 2018.
  41. Garmes HM, Carvalheira JBC, Reis F, Queiroz LS, Fabbro MD, Souza VFP, et al. Pituitary carcinoma: A case report and discussion of potential value of combined use of Ga-68 DOTATATE and F-18 FDG PET/CT scan to better choose therapy. *Surg Neurol Int.* 2017;8:162, <http://dx.doi.org/10.4103/sni.sni.498.16>.
  42. Novruzov F, Aliyev JA, Jaunmuktane Z, Bomanji JB, Kayani I. The use of (68)Ga DOTATATE PET/CT for diagnostic assessment and monitoring of (177)Lu DOTATATE therapy in pituitary carcinoma. *Clin Nucl Med.* 2015;40:47–9, <http://dx.doi.org/10.1097/rlu.0000000000000589>.
  43. Manara R, Maffei P, Citton V, Rizzati S, Bommarito G, Ermani M, et al. Increased rate of intracranial saccular aneurysms in acromegaly: An mr angiography study and review of the literature. *J Clin Endocrinol Metab.* 2011;96:1292–300, <http://dx.doi.org/10.1210/jc.2010-2721>.
  44. Linn J, Peters F, Lummel N, Schankin C, Rächinger W, Brueckmann H, et al. Detailed imaging of the normal anatomy and pathologic conditions of the cavernous region at 3 Tesla using a contrast-enhanced

- MR angiography. *Neuroradiology*. 2011;53:947–54, <http://dx.doi.org/10.1007/s00234-011-0837-3>.
45. Hardy J, Vezina JL. Transsphenoidal neurosurgery of intracranial neoplasm. *Adv Neurol*. 1976;15:261–73.
  46. Knosp E, Steiner E, Kitz K, Matula C. Pituitary adenomas with invasion of the cavernous sinus space: A magnetic resonance imaging classification compared with surgical findings. *Neurosurgery*. 1993;33:610–7, <http://dx.doi.org/10.1227/00006123-199310000-00008> [discussion 7–8].
  47. Micko AS, Wohrer A, Wolfsberger S, Knosp E. Invasion of the cavernous sinus space in pituitary adenomas: Endoscopic verification and its correlation with an MRI-based classification. *J Neurosurg*. 2015;122:803–11, <http://dx.doi.org/10.3171/2014.12.JNS141083>.
  48. Anik I, Cabuk B, Gokbel A, Selek A, Cetinarlan B, Anik Y, et al. Endoscopic Transsphenoidal approach for acromegaly with remission rates in 401 patients: 2010 Consensus Criteria. *World Neurosurg*. 2017;108:278–90, <http://dx.doi.org/10.1016/j.wneu.2017.08.182>.
  49. Brochier S, Galland F, Kujas M, Parker F, Gaillard S, Raftopoulos C, et al. Factors predicting relapse of non-functioning pituitary macroadenomas after neurosurgery: A study of 142 patients. *Eur J Endocrinol*. 2010;163:193–200, <http://dx.doi.org/10.1530/EJE-10-0255>.
  50. Galm BP, Martinez-Salazar EL, Swearingen B, Torriani M, Klibanski A, Bredella MA, et al. MRI texture analysis as a predictor of tumor recurrence or progression in patients with clinically non-functioning pituitary adenomas. *Eur J Endocrinol*. 2018;179:191–8, <http://dx.doi.org/10.1530/EJE-18-0291>.
  51. Black PM, Moriarty T, Alexander E 3rd, Stieg P, Woodard EJ, Gleason PL, et al. Development and implementation of intraoperative magnetic resonance imaging and its neurosurgical applications. *Neurosurgery*. 1997;41:831–42, <http://dx.doi.org/10.1097/00006123-199710000-00013> [discussion 42–45].
  52. Buchfelder M, Schlaffer SM. Intraoperative magnetic resonance imaging for pituitary adenomas. *Front Horm Res*. 2016;45:121–32, <http://dx.doi.org/10.1159/000442328>.
  53. Yoon PH, Kim DI, Jeon P, Lee SI, Lee SK, Kim SH. Pituitary adenomas: Early postoperative MR imaging after transsphenoidal resection. *AJNR Am J Neuroradiol*. 2001;22:1097–104.
  54. Kiliç T, Ekinci G, Seker A, Elmaci I, Erzen C, Pamir MN. Determining optimal MRI follow-up after transsphenoidal surgery for pituitary adenoma: Scan at 24 hours postsurgery provides reliable information. *Acta Neurochir (Wien)*. 2001;143:1103–26, <http://dx.doi.org/10.1007/s007010100002>.
  55. Taberner Lopez E, Vano Molina M, Calatayud Gregori J, Jornet Sanz M, Jornet Fayos J, Pastor Del Campo A, et al. Assessment of the extent of pituitary macroadenomas resection in immediate postoperative MRI. *Radiologia*. 2018;60:64–72, <http://dx.doi.org/10.1016/j.rx.2017.10.008>.
  56. Stofko DL, Nickles T, Sun H, Dehdashti AR. The value of immediate postoperative MR imaging following endoscopic endonasal pituitary surgery. *Acta Neurochir (Wien)*. 2014;156:133–40, <http://dx.doi.org/10.1007/s00701-013-1834-6> [discussion 40].
  57. Kim HY, Kim ST, Kim HJ, Jeon P, Byun HS, Kim YK, et al. Differentiation of postoperative changes and residual tumors in dynamic contrast-enhanced sella MRI after transsphenoidal resection of pituitary adenoma. *Medicine (Baltimore)*. 2019;98:e16089, <http://dx.doi.org/10.1097/md.000000000016089>.
  58. Cortet-Rudelli C, Bonneville JF, Borson-Chazot F, Clavier L, Coche Dequeant B, Desailly R, et al. Post-surgical management of non-functioning pituitary adenoma. *Ann Endocrinol (Paris)*. 2015;76:228–38, <http://dx.doi.org/10.1016/j.ando.2015.04.003>.
  59. Hughes JD, Koeller K, Rinaldo L, Erickson D, Bancos I, Meyer FB, et al. Beyond gross total and subtotal: Does volumetric resection matter in nonfunctioning pituitary macroadenomas? *World Neurosurg*. 2018;116:e733–7, <http://dx.doi.org/10.1016/j.wneu.2018.05.077>.
  60. Wass JA, Reddy R, Karavitaki N. The postoperative monitoring of nonfunctioning pituitary adenomas. *Nat Rev Endocrinol*. 2011;7:431–4, <http://dx.doi.org/10.1038/nrendo.2011.54>.
  61. Brada M, Jankowska P. Radiotherapy for pituitary adenomas. *Endocrinol Metab Clin North Am*. 2008;37:263–75, <http://dx.doi.org/10.1016/j.ecl.2007.10.005>, xi.
  62. Minniti G, Osti MF, Niyazi M. Target delineation and optimal radiosurgical dose for pituitary tumors. *Radiat Oncol*. 2016;11:135, <http://dx.doi.org/10.1186/s13014-016-0710-y>.
  63. Koulouri O, Kandasamy N, Hoole AC, Gillett D, Heard S, Powlson AS, et al. Successful treatment of residual pituitary adenoma in persistent acromegaly following localisation by 11C-methionine PET co-registered with MRI. *Eur J Endocrinol*. 2016;175:485–98, <http://dx.doi.org/10.1530/EJE-16-0639>.
  64. d'Amico A, Stapor-Fudzinska M, Tarnawski R. CyberKnife radiosurgery planning of a secreting pituitary adenoma performed with (6)(8)Ga DOTATATE PET and MRI. *Clin Nucl Med*. 2014;39:1043–4, <http://dx.doi.org/10.1097/RLU.0000000000000535>.
  65. Taku N, Koulouri O, Scoffings D, Gurnell M, Burnet N. The use of (11)carbon methionine positron emission tomography (PET) imaging to enhance radiotherapy planning in the treatment of a giant, invasive pituitary adenoma. *BJR Case Rep*. 2017;3:20160098, <http://dx.doi.org/10.1259/bjrcr.20160098>.
  66. Wang H, Hou B, Lu L, Feng M, Zang J, Yao S, et al. PET/MRI in the Diagnosis of Hormone-Producing Pituitary Microadenoma: A Prospective Pilot Study. *J Nucl Med*. 2018;59:523–8, <http://dx.doi.org/10.2967/jnumed.117.191916>.
  67. Trouillas J, Roy P, Sturm N, Dantony E, Cortet-Rudelli C, Viennet G, et al. A new prognostic clinicopathological classification of pituitary adenomas: a multicentric case-control study of 410 patients with 8 years postoperative follow-up. *Acta Neuropathol*. 2013;126:123–35, <http://dx.doi.org/10.1007/s00401-013-1084-y>.
  68. Vasiljevic A, Jouanneau E, Trouillas J, Raverot G. Clinicopathological prognostic and theranostic markers in pituitary tumors. *Minerva Endocrinol*. 2016;41:377–89.
  69. Alhambra-Exposito MR, Ibanez-Costa A, Moreno-Moreno P, Rivero-Cortes E, Vazquez-Borrego MC, Blanco-Acevedo C, et al. Association between radiological parameters and clinical and molecular characteristics in human somatotropinomas. *Sci Rep*. 2018;8:6173, <http://dx.doi.org/10.1038/s41598-018-24260-y>.
  70. Cuevas-Ramos D, Carmichael JD, Cooper O, Bonert VS, Gertych A, Mamelak AN, et al. A Structural and Functional Acromegaly Classification. *The Journal of Clinical Endocrinology & Metabolism*. 2015;100:122–31, <http://dx.doi.org/10.1210/jc.2014-2468>.
  71. Puig Domingo M. Treatment of acromegaly in the era of personalized and predictive medicine. *Clin Endocrinol (Oxf)*. 2015;83:3–14, <http://dx.doi.org/10.1111/cen.12731>.
  72. Puig-Domingo M, Marazuela M. Precision medicine in the treatment of acromegaly. *Minerva Endocrinol*. 2019;44:169–75, <http://dx.doi.org/10.23736/s0391-1977.18.02937-1>.
  73. Puig-Domingo M, Resmini E, Gomez-Anson B, Nicolau J, Mora M, Palomera E, et al. Magnetic resonance imaging as a predictor of response to somatostatin analogs in acromegaly after surgical failure. *J Clin Endocrinol Metab*. 2010;95:4973–8, <http://dx.doi.org/10.1210/jc.2010-0573>.
  74. Wang S, Lin K, Xiao D, Wei L, Zhao L. The Relationship Between Posterior Pituitary Bright Spot on Magnetic Resonance Imaging (MRI) and Postoperative Diabetes Insipidus for



- Pituitary Adenoma Patients. *Med Sci Monit.* 2018;24:6579–86, <http://dx.doi.org/10.12659/MSM.908349>.
75. Surov A, Meyer HJ, Wienke A. Associations between apparent diffusion coefficient (ADC) and KI 67 in different tumors: a meta-analysis. Part 1: ADCmean. *Oncotarget.* 2017;8:75434–44, <http://dx.doi.org/10.18632/oncotarget.20406>.
  76. Tamrazi B, Pekmezci M, Aboian M, Tihan T, Glastonbury CM. Apparent diffusion coefficient and pituitary macroadenomas: pre-operative assessment of tumor atypia. *Pituitary.* 2017;20:195–200, <http://dx.doi.org/10.1007/s11102-016-0759-5>.
  77. Bonneville J-F. *The Pituitary Gland After Radiation Therapy.* In: *MRI of the Pituitary Gland.* Cham: Springer International Publishing; 2016. p. 205–9.
  78. Azab WA, Nasim K, Abdelnabi EA, Yousef W, Najibullah M, Khan T, et al. Endoscopic Endonasal Excision of Large and Giant Pituitary Adenomas: Radiological and Intraoperative Correlates of the Extent of Resection. *World Neurosurg.* 2019;126:e793–802, <http://dx.doi.org/10.1016/j.wneu.2019.02.151>.
  79. Kopp C, Theodorou M, Poullos N, Jacob V, Astner ST, Molls M, et al. Tumor shrinkage assessed by volumetric MRI in long-term follow-up after fractionated stereotactic radiotherapy of nonfunctioning pituitary adenoma. *Int J Radiat Oncol Biol Phys.* 2012;82:1262–7, <http://dx.doi.org/10.1016/j.ijrobp.2011.02.053>.
  80. Hagiwara A, Inoue Y, Wakasa K, Haba T, Tashiro T, Miyamoto T. Comparison of growth hormone-producing and non-growth hormone-producing pituitary adenomas: imaging characteristics and pathologic correlation. *Radiology.* 2003;228:533–8, <http://dx.doi.org/10.1148/radiol.2282020695>.
  81. Heck A, Ringstad G, Fougner SL, Casar-Borota O, Nome T, Ramm-Petersen J, et al. Intensity of pituitary adenoma on T2-weighted magnetic resonance imaging predicts the response to octreotide treatment in newly diagnosed acromegaly. *Clin Endocrinol (Oxf).* 2012;77:72–8, <http://dx.doi.org/10.1111/j.1365-2265.2011.04286.x>.
  82. Heck A, Emblem KE, Casar-Borota O, Bollerslev J, Ringstad G. Quantitative analyses of T2-weighted MRI as a potential marker for response to somatostatin analogs in newly diagnosed acromegaly. *Endocrine.* 2016;52:333–43, <http://dx.doi.org/10.1007/s12020-015-0766-8>.
  83. Heck A, Emblem KE, Casar-Borota O, Ringstad G, Bollerslev J. MRI T2 characteristics in somatotroph adenomas following somatostatin analog treatment in acromegaly. *Endocrine.* 2016;53:327–30, <http://dx.doi.org/10.1007/s12020-015-0816-2>.
  84. Potorac I, Petrossians P, Daly AF, Alexopoulou O, Borot S, Sahnoun-Fathallah M, et al. T2-weighted MRI signal predicts hormone and tumor responses to somatostatin analogs in acromegaly. *Endocr Relat Cancer.* 2016;23:871–81, <http://dx.doi.org/10.1530/ERC-16-0356>.
  85. Ezzat S, Caspar-Bell GM, Chik CL, Denis MC, Domingue ME, Imran SA, et al. Predictive Markers for Postsurgical Medical Management of Acromegaly: A Systematic Review and Consensus Treatment Guideline. *Endocr Pract.* 2019;25:379–93, <http://dx.doi.org/10.4158/EP-2018-0500>.
  86. Burlacu MC, Maiter D, Duprez T, Delgrange E. T2-weighted magnetic resonance imaging characterization of prolactinomas and association with their response to dopamine agonists. *Endocrine.* 2019;63:323–31, <http://dx.doi.org/10.1007/s12020-018-1765-3>.
  87. Kreutz J, Vroonen L, Cattin F, Petrossians P, Thiry A, Rostomyan L, et al. Intensity of prolactinoma on T2-weighted magnetic resonance imaging: towards another gender difference. *Neuroradiology.* 2015;57:679–84, <http://dx.doi.org/10.1007/s00234-015-1519-3>.
  88. Levine SN, Ishaq S, Nanda A, Wilson JD, Gonzalez-Toledo E. Occurrence of extensive spherical amyloid deposits in a prolactin-secreting pituitary macroadenoma: a radiologic-pathologic correlation. *Ann Diagn Pathol.* 2013;17:361–6, <http://dx.doi.org/10.1016/j.anndiagpath.2013.03.001>.
  89. Varlamov EV, Hinojosa-Amaya JM, Fleseriu M. Magnetic resonance imaging in the management of prolactinomas; a review of the evidence. *Pituitary.* 2020;23:16–26, <http://dx.doi.org/10.1007/s11102-019-01001-6>.
  90. Dogansen SC, Yalin GY, Tanrikulu S, Tekin S, Nizam N, Bilgic B, et al. Clinicopathological significance of baseline T2-weighted signal intensity in functional pituitary adenomas. *Pituitary.* 2018;21:347–54, <http://dx.doi.org/10.1007/s11102-018-0877-3>.
  91. Biagetti B, Sarria-Estrada S, Ng-Wong YK, Martinez-Saez E, Casteràs A, Cordero Asanza E, et al. Shrinkage by the third month predicts long-term response of macroprolactinoma after cabergoline. *Eur J Endocrinol.* 2021;185:587–95, <http://dx.doi.org/10.1530/eje-21-0561>.
  92. Kurosaki M, Kambe A, Watanabe T, Fujii S, Ogawa T. Serial 3 T magnetic resonance imaging during cabergoline treatment of macroprolactinomas. *Neurol Res.* 2015;37:341–6, <http://dx.doi.org/10.1179/1743132814Y.0000000457>.
  93. Faje A, Chunharojrith P, Nancy J, Biller BMK, Swearingen B, Klibanski A. Dopamine Agonists Can Reduce Cystic Prolactinomas. *The Journal of Clinical Endocrinology & Metabolism.* 2016;101:3709–15, <http://dx.doi.org/10.1210/jc.2016-2008>.
  94. Eroukhanoff J, Tejedor I, Potorac I, Cuny T, Bonneville JF, Dufour H, et al. MRI follow-up is unnecessary in patients with macroprolactinomas and long-term normal prolactin levels on dopamine agonist treatment. *Eur J Endocrinol.* 2017;176:323–8, <http://dx.doi.org/10.1530/EJE-16-0897>.
  95. Alkabbani AG, Mon SY, Hatipoglu B, Kennedy L, Faïman C, Weil RJ, et al. Is a stable or decreasing prolactin level in a patient with prolactinoma a surrogate marker for lack of tumor growth? *Pituitary.* 2014;17:97–102, <http://dx.doi.org/10.1007/s11102-013-0473-5>.
  96. Rodriguez-Barcelo S, Gutierrez-Cardo A, Dominguez-Paez M, Medina-Imbroda J, Romero-Moreno L, Arraez-Sanchez M. Clinical usefulness of coregistered 11C-methionine positron emission tomography/3-T magnetic resonance imaging at the follow-up of acromegaly. *World Neurosurg.* 2014;82:468–73, <http://dx.doi.org/10.1016/j.wneu.2013.11.011>.
  97. Seriola S, Doglietto F, Fiorindi A, Biroli A, Mattavelli D, Buffoli B, et al. Pituitary adenomas and invasiveness from anatomic-surgical, radiological, and histological perspectives: A systematic literature review. *Cancers.* 2019;11:1936.
  98. Batista D, Courkoutsakis NA, Oldfield EH, Griffin KJ, Keil M, Patronas NJ, et al. Detection of adrenocorticotropin-secreting pituitary adenomas by magnetic resonance imaging in children and adolescents with cushing disease. *J Clin Endocrinol Metab.* 2005;90:5134–40, <http://dx.doi.org/10.1210/jc.2004-1778>.
  99. Patronas N, Bulakbasi N, Stratakis CA, Lafferty A, Oldfield EH, Doppman J, et al. Spoiled gradient recalled acquisition in the steady state technique is superior to conventional postcontrast spin echo technique for magnetic resonance imaging detection of adrenocorticotropin-secreting pituitary tumors. *J Clin Endocrinol Metab.* 2003;88:1565–9, <http://dx.doi.org/10.1210/jc.2002-021438>.
  100. Grober Y, Grober H, Wintermark M, Jane JA, Oldfield EH. Comparison of MRI techniques for detecting microadenomas in Cushing's disease. *J Neurosurg.* 2018;128:1051–7, <http://dx.doi.org/10.3171/2017.3.JNS163122>.
  101. Chatain GP, Patronas N, Smirniotopoulos JG, Piazza M, Benzo S, Ray-Chaudhury A, et al. Potential utility of FLAIR in MRI-negative Cushing's disease. *J Neurosurg.* 2018;129:620–8, <http://dx.doi.org/10.3171/2017.4.JNS17234>.



102. Rogg JM, Tung GA, Anderson G, Cortez S. Pituitary apoplexy: early detection with diffusion-weighted MR imaging. *AJNR Am J Neuroradiol.* 2002;23:1240–5.
103. Kunii N, Abe T, Kawamo M, Tanioka D, Izumiyama H, Moritani T. Rathke's cleft cysts: Differentiation from other cystic lesions in the pituitary fossa by use of single-shot fast spin-echo diffusion-weighted MR imaging. *Acta Neurochir (Wien).* 2007;149:759–69, <http://dx.doi.org/10.1007/s00701-007-1234-x>.
104. Khant ZA, Azuma M, Kadota Y, Hattori Y, Takeshima H, Yokogami K, et al. Evaluation of pituitary structures and lesions with turbo spin-echo diffusion-weighted imaging. *J Neurol Sci.* 2019;405:116390, <http://dx.doi.org/10.1016/j.jns.2019.07.008>.
105. Snow RB, Lavyne MH, Lee BC, Morgello S, Patterson RH Jr. Craniotomy versus transsphenoidal excision of large pituitary tumors: the usefulness of magnetic resonance imaging in guiding the operative approach. *Neurosurgery.* 1986;19:59–64, <http://dx.doi.org/10.1227/00006123-198607000-00008>.
106. Iuchi T, Saeki N, Tanaka M, Sunami K, Yamaura A. MRI prediction of fibrous pituitary adenomas. *Acta Neurochir (Wien).* 1998;140:779–86, <http://dx.doi.org/10.1007/s007010050179>.
107. Yu CS, Li KC, Xuan Y, Ji XM, Qin W. Diffusion tensor tractography in patients with cerebral tumors: A helpful technique for neurosurgical planning and post-operative assessment. *Eur J Radiol.* 2005;56:197–204, <http://dx.doi.org/10.1016/j.ejrad.2005.04.010>.
108. Salmela MB, Cauley KA, Nickerson JP, Koski CJ, Filippi CG. Magnetic resonance diffusion tensor imaging (MRDTI) and tractography in children with septo-optic dysplasia. *Pediatric Radiology.* 2010;40:708–13, <http://dx.doi.org/10.1007/s00247-009-1478-0>.
109. Anik I, Anik Y, Cabuk B, Caklili M, Pirhan D, Ozturk O, et al. Visual outcome of an endoscopic endonasal transsphenoidal approach in pituitary macroadenomas: Quantitative assessment with diffusion tensor imaging early and long-term results. *World Neurosurg.* 2018;112:e691–701, <http://dx.doi.org/10.1016/j.wneu.2018.01.134>.
110. Doai M, Tonami H, Matoba M, Tachibana O, Iizuka H, Nakada S, et al. Pituitary macroadenoma: Accuracy of apparent diffusion coefficient magnetic resonance imaging in grading tumor aggressiveness. *Neuroradiol J.* 2019;32:86–91, <http://dx.doi.org/10.1177/1971400919825696>.
111. Pierallini A, Caramia F, Falcone C, Tinelli E, Paonessa A, Ciddio AB, et al. Pituitary macroadenomas: Preoperative evaluation of consistency with diffusion-weighted MR imaging—initial experience. *Radiology.* 2006;239:223–31, <http://dx.doi.org/10.1148/radiol.2383042204>.
112. Wang M, Liu H, Wei X, Liu C, Liang T, Zhang X, et al. Application of reduced-FOV diffusion-weighted imaging in evaluation of normal pituitary glands and pituitary macroadenomas. *Am J Neuroradiol.* 2018;39:1499–504, <http://dx.doi.org/10.3174/ajnr.A5735>.
113. Yiping L, Ji X, Daoying G, Bo Y. Prediction of the consistency of pituitary adenoma: A comparative study on diffusion-weighted imaging and pathological results. *J Neuroradiol.* 2016;43:186–94, <http://dx.doi.org/10.1016/j.neurad.2015.09.003>.
114. Mahmoud OM, Tominaga A, Amaty VJ, Ohtaki M, Sugiyama K, Sakoguchi T, et al. Role of PROPELLER diffusion-weighted imaging and apparent diffusion coefficient in the evaluation of pituitary adenomas. *Eur J Radiol.* 2011;80:412–7, <http://dx.doi.org/10.1016/j.ejrad.2010.05.023>.
115. Sanei Taheri M, Kimia F, Mehrnahad M, Saligheh Rad H, Haghhighatkhah H, Moradi A, et al. Accuracy of diffusion-weighted imaging-magnetic resonance in differentiating functional from non-functional pituitary macro-adenoma and classification of tumor consistency. *Neuroradiol J.* 2019;32:74–85, <http://dx.doi.org/10.1177/1971400918809825>.
116. Suzuki C, Maeda M, Hori K, Kozuka Y, Sakuma H, Taki W, et al. Apparent diffusion coefficient of pituitary macroadenoma evaluated with line-scan diffusion-weighted imaging. *J Neuroradiol.* 2007;34:228–35, <http://dx.doi.org/10.1016/j.neurad.2007.06.007>.
117. Boxerman JL, Rogg JM, Donahue JE, Machan JT, Goldman MA, Doberstein CE. Preoperative MRI evaluation of pituitary macroadenoma: Imaging features predictive of successful transsphenoidal surgery. *AJR Am J Roentgenol.* 2010;195:720–8, <http://dx.doi.org/10.2214/AJR.09.4128>.
118. Hassan HA, Bessar MA, Herzallah IR, Laury AM, Arnaout MM, Basha MAA. Diagnostic value of early postoperative MRI and diffusion-weighted imaging following trans-sphenoidal resection of non-functioning pituitary macroadenomas. *Clin Radiol.* 2018;73:535–41, <http://dx.doi.org/10.1016/j.crad.2017.12.007>.
119. Ma Z, He W, Zhao Y, Yuan J, Zhang Q, Wu Y, et al. Predictive value of PWI for blood supply and T1-spin echo MRI for consistency of pituitary adenoma. *Neuroradiology.* 2016;58:51–7, <http://dx.doi.org/10.1007/s00234-015-1591-8>.
120. Bładowska J, Zimny A, Guziński M, Hałoń A, Tabakow P, Czyż M, et al. Usefulness of perfusion weighted magnetic resonance imaging with signal-intensity curves analysis in the differential diagnosis of sellar and parasellar tumors: Preliminary report. *Eur J Radiol.* 2013;82:1292–8, <http://dx.doi.org/10.1016/j.ejrad.2013.01.033>.
121. Hakyemez B, Yildirim N, Erdoğan C, Kocaeli H, Korfali E, Parlak M. Meningiomas with conventional MRI findings resembling intraaxial tumors: Can perfusion-weighted MRI be helpful in differentiation? *Neuroradiology.* 2006;48:695–702, <http://dx.doi.org/10.1007/s00234-006-0115-y>.
122. Pinzariu O, Georgescu B, Georgescu CE. Metabolomics-A promising approach to pituitary adenomas. *Front Endocrinol (Lausanne).* 2018;9:814, <http://dx.doi.org/10.3389/fendo.2018.00814>.
123. Chernov MF, Kawamata T, Amano K, Ono Y, Suzuki T, Nakamura R, et al. Possible role of single-voxel 1H-MRS in differential diagnosis of suprasellar tumors. *J Neurooncol.* 2009;91:191–8, <http://dx.doi.org/10.1007/s11060-008-9698-y>.
124. Einstien A, Virani RA. Clinical relevance of single-voxel (1)H MRS metabolites in discriminating suprasellar tumors. *J Clin Diagn Res.* 2016;10:TC01–4, <http://dx.doi.org/10.7860/JCDR/2016/17988.8078>.
125. Bou-Ayache JM, Delman BN. Advances in imaging of the pediatric pituitary gland. *Endocrinol Metab Clin North Am.* 2016;45:443–52, <http://dx.doi.org/10.1016/j.ecl.2016.02.004>.
126. Chapman PR, Singhal A, Gaddamanugu S, Prattipati V. Neuroimaging of the pituitary gland: Practical anatomy and pathology. *Radiol Clin North Am.* 2020;58:1115–33, <http://dx.doi.org/10.1016/j.rcl.2020.07.009>.
127. Hu J, Yan J, Zheng X, Zhang Y, Ran Q, Tang X, et al. Magnetic resonance spectroscopy may serve as a presurgical predictor of somatostatin analog therapy response in patients with growth hormone-secreting pituitary macroadenomas. *J Endocrinol Invest.* 2019;42:443–51, <http://dx.doi.org/10.1007/s40618-018-0939-4>.
128. Hughes JD, Fattahi N, Van Gompel J, Arani A, Ehman R, Huston J. Magnetic resonance elastography detects tumoral consistency in pituitary macroadenomas. *Pituitary.* 2016;19:286–92, <http://dx.doi.org/10.1007/s11102-016-0706-5>.
129. Sakai N, Takehara Y, Yamashita S, Ohishi N, Kawaji H, Sameshima T, et al. Shear stiffness of 4 common intracranial tumors measured using MR elastography: comparison with

- intraoperative consistency grading. *AJNR Am J Neuroradiol.* 2016;37:1851–9, <http://dx.doi.org/10.3174/ajnr.A4832>.
130. Lang M, Habboub G, Moon D, Bandyopadhyay A, Silva D, Kennedy L, et al. Comparison of constructive interference in steady-state and T1-weighted MRI sequence at detecting pituitary adenomas in Cushing's disease patients. *J Neurol Surg B Skull Base.* 2018;79:593–8, <http://dx.doi.org/10.1055/s-0038-1642032>.
131. Yamamoto J, Kakeda S, Shimajiri S, Takahashi M, Watanabe K, Kai Y, et al. Tumor consistency of pituitary macroadenomas: predictive analysis on the basis of imaging features with contrast-enhanced 3D FIESTA at 3T. *Am J Neuroradiol.* 2014;35:297–303, <http://dx.doi.org/10.3174/ajnr.A3667>.
132. Watanabe K, Kakeda S, Yamamoto J, Watanabe R, Nishimura J, Ohnari N, et al. Delineation of optic nerves and chiasm in close proximity to large suprasellar tumors with contrast-enhanced FIESTA MR imaging. *Radiology.* 2012;264:852–8, <http://dx.doi.org/10.1148/radiol.12111363>.